Correlation of Water Exchange Rate with Isomeric Composition in Diastereoisomeric Gadolinium Complexes of Tetra(carboxyethyl)dota and Related Macrocyclic Ligands

Mark Woods,[†] Silvio Aime,[‡] Mauro Botta,[§] Judith A. K. Howard,[†] Janet M. Moloney,[†] Michel Navet,[||] David Parker,*[,||] Marc Port, and Olivier Rousseaux[||]

Contribution from the Department of Chemistry, University of Durham, South Road, Durham, DH1 3LE, U.K., the Dipartimento di Chimica I.F.M., Universita di Torino, via P. Giuria 7, 10125 Torino, Italy, Dipartimento di Scienze e Tecnologie Avanzate, Universita del Piemonte Orientale "Amedeo Avogadro", Corso Borsalino 54, 10131 Alessandria, and Guerbet s.a., Aulnay-sous-Bois, 95943 Roissy-Charles de Gaulle, France

Received December 23, 1999. Revised Manuscript Received July 26, 2000

Abstract: The solution structure and dynamics of metal-bound water exchange have been studied in a series of diastereoisomeric gadolinium complexes of tetra(carboxyethyl) derivatives of 1,4,7,10-tetraazacyclodecane. The structures of the (*RRRS*), (*RSRS*), and (*RRSS*) ligands and the Eu, Gd, and Tb complexes of the (*RRRR*) isomer have been determined by X-ray crystallography. Luminescence measurements on the Eu and Tb complexes revealed an integral hydration state ($q = 1$) in each case for the Eu isomers, whereas nonintegral values were measured for the (*RRRR*) and (*RRRS*) Tb isomers (e.g., [(*RRRR*)-Tb·**1**]$^-$, $q = 0.60$). The ratio of the twisted and regular monocapped square antiprismatic isomers has been measured in solution by ^{1}H NMR for the Eu and Tb complexes and followed the order, (*RRRR*) > (*RRRS*) > (*RSRS*) > (*RRSS*). Water exchange rates in the gadolinium complexe have been determined by ^{17}O NMR and were fastest for the (*RRRR*) isomer [$\tau_m = 68$ ns (298 K)] and correlated very well with the proportion of the twisted square anti-prismatic isomer. The rate of water exchange in the (*RRRR*) Gd complexes is likely to be sufficiently fast so as not to limit the overall relaxivity in higher MW conjugates.

Introduction

The majority of the paramagnetic contrast agents used in diagnostic MRI procedures use complexes of gadolinium. While there are now several low molecular weight paramagnetic contrast agents available for clinical use,[1] the development of higher relaxivity contrast agents, in which the paramagnetic center is directly conjugated or noncovalently bound to a higher molecular weight vector, has occurred at a slower rate. The reasons for this are 2-fold: first, the motion of the paramagnetic center is usually not efficiently coupled to the motion of the more slowly tumbling macromolecule so that the effective correlation time of the paramagnetic center (τ_r) is less than it could be.[1,2] Second, the rate of water proton exchange ($1/\tau_m$) may not be sufficiently fast so as to avoid it limiting the measured relaxivity.[3−5] Recent studies have served to highlight the important role of the rate of water exchange:[6] in the absence of prototropic exchange, it determines the efficiency of the transfer of paramagnetism to bulk water protons and also contributes to the modulation of the electron-nucleus dipolar interaction. In Solomon−Bloembergen−Morgan theory,[1] the inner-sphere contribution to the measured water proton relaxation rate is given by eq 1, where q is the number of metal-

$$R_{1p} = \frac{C_{tot}q}{55.6}\left(\frac{1}{T_{1m} + \tau_m}\right) \quad (1)$$

bound water molecules, C_{tot} is the molar concentration of the paramagnetic complex, and T_{1m} is the longitudinal water proton relaxation time. When $\tau_m > T_{1m}$, i.e., when the water of exchange rate becomes slower, then τ_m may determine the inner-sphere relaxivity contribution. Examples of such systems range from charge neutral complexes of DTPA-diamides—where the effect is somewhat marginal[5]—to cationic tetraamide gadolinium

[†] University of Durham.
[‡] Universita degli Studi di Torino.
[§] Universita del Piemonte Orientale "Amedeo Avogadro".
[||] Guerbet s.a.

(1) (a) Aime, S.; Botta, M.; Fasano, M.; Terreno, M. *Chem. Soc. Rev.* **1998**, *27*, 19. (b) Peters, J. A.; Huskens, J.; Raber, D. J. *Prog. NMR Spectrosc.* **1996**, *28*, 283. (c) Lauffer, R. B. *Chem. Rev.* **1987**, *87*, 901. (d) Caravan, P.; Ellison, J.; McMurry, T. J.; Lauffer, R. B. *Chem. Rev.* **1999**, *99*, 2293.

(2) (a) Parker, D.; Williams, J. A. G. *J. Chem. Soc., Dalton Trans.* **1996**, 3613. (b) Lauffer, R. B.; Brady, T. J. *Magn. Reson. Imaging* **1985**, *3*, 11. (c) Lauffer, R. B.; Brady, T. J.; Brown, R. D.; Baglin, C.; Koenig, S. H. *Magn. Reson. Med.* **1986**, *3*, 541. (d) Aime, S.; Botta, M.; Fasano, M.; Crich, S. G.; Terreno, E. *J. Biol. Inorg. Chem.* **1996**, 312. (e) Koenig, S. H. *Invest. Radiol.* **1994**, *29*, 5128.

(3) Meiboom, S. *J. Chem. Phys.* **1961**, *34*, 375. (b) Frey, U.; Merbach, A. E.; Powell, D. H. In *Dynamics of Solutions and Fluid Mixtures by NMR*; Delpuech, J.-J., Ed.; John Wiley & Sons Ltd.: Chichester, 1995; pp 263−307.

(4) Cossy, C.; Helm, A. E.; Merbach, A. E. *Inorg. Chem.* **1988**, *27*, 1973.

(5) (a) Gonzalez, G.; Powell, D. H.; Tissières, V.; Merbach, A. E. *J. Phys. Chem.* **1994**, *98*, 53. (b) Aime, S.; Botta, M.; Fasano, M.; Paoletti, S.; Anelli, P. L.; Uggeri, F.; Virtuani, M. *Inorg. Chem.* **1994**, *33*, 4707.

(6) (a) Aime, S.; Barge, A.; Botta, M.; Parker, D.; de Sousa, A. S. *J. Am. Chem. Soc* **1997**, *119*, 4767. (b) Aime, S.; Barge, A.; Botta, M.; Parker, D.; de Sousa, A. S. *Angew Chem. Int. Ed. Engl.* **1998**, *37*, 2673. (c) Batsanov, A. S.; Beeby, A.; Bruce, J. I., Howard, J. A. K., Kenwright, A. M.; Parker, D. *Chem. Commun.* **1999**, 1011. (d) Aime, S.; Barge, A.; Bruce, J. I.; Botta, M.; Howard, J. A. K.; Moloney, J. M.; Parker, D.; de Sousa, A. S.; Woods, M. *J. Am. Chem. Soc.* **1999**, *121*, 5762. (e) Aime, S.; Botta, M.; Ermondi, G.; Fedeli, F.; Uggeri, F. *Inorg. Chem.* **1992**, *31*, 1100.

10.1021/ja994492v CCC: $19.00
Published on Web 09/21/2000

Chart 1

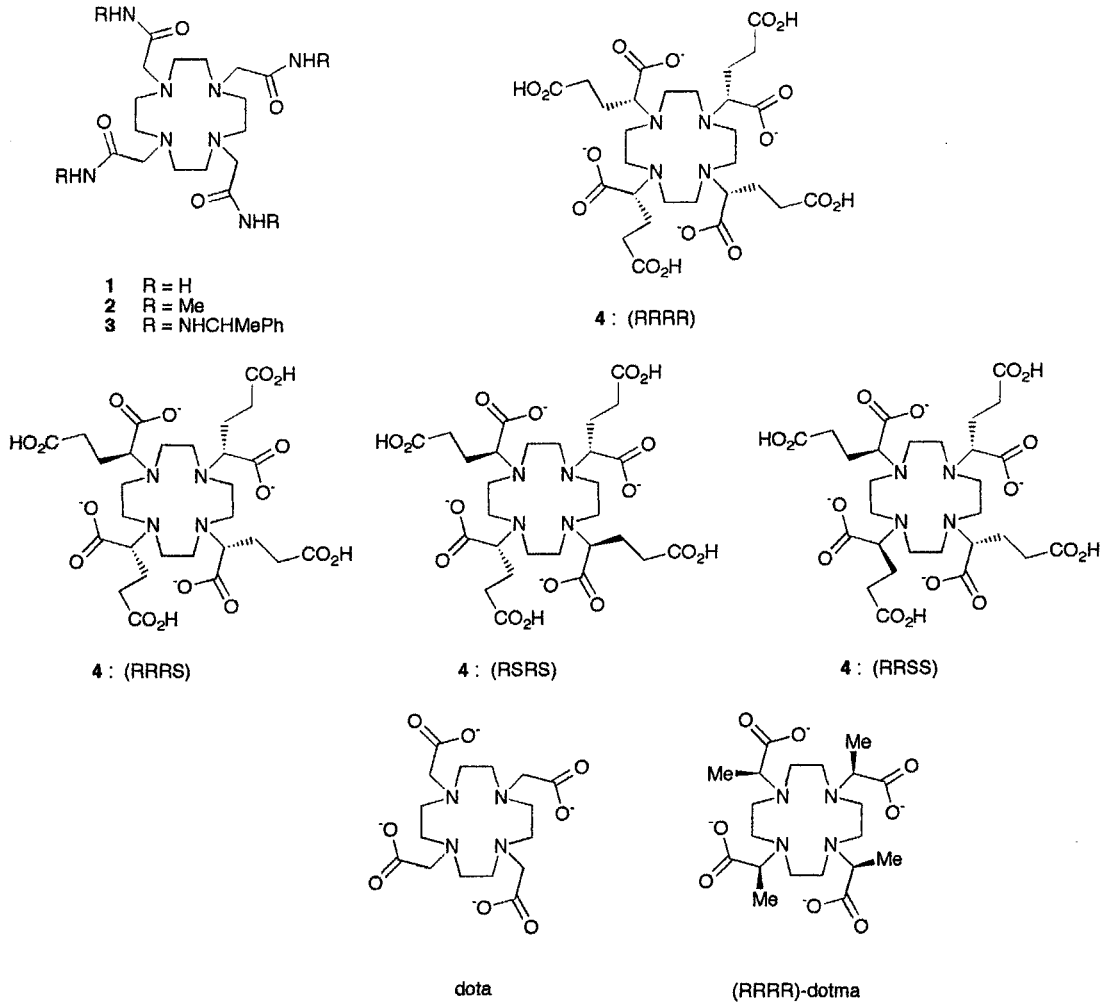

Scheme 1

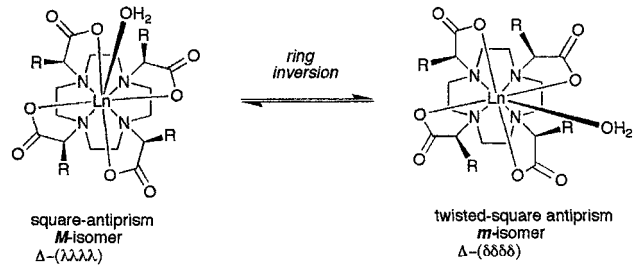

complexes, in which τ_m is of the order of 15−20 μs at 298 K and the overall relaxivity at ambient pH is almost entirely due to the outer-sphere contribution, R_{1p}^{os} (eq 2).[6]

$$R_{1p} = R_{1p}^{is} + R_{1p}^{os} \quad (2)$$

Very recently it was elegantly demonstrated by NMR and luminescence studies that the rate of water exchange at lanthanide ions (e.g., Eu and Yb) is dependent upon the nature and composition of the isomers of a given complex.[6b−d] Thus, for europium complexes of tetraamides **1**−**3** (see Chart 1), the rate of water exchange at 298 K is the order of 6×10^3 s^{-1} at 298 K for the major square antiprismatic isomer (M; Scheme 1) but some 50 times faster in the isomeric, twisted square-antiprismatic isomer (m). Exchange between these two isomers occurs either by cooperative ring inversion ($\lambda \rightarrow \delta$ in each five-ring NCCN chelate) or concerted arm rotation ($\Delta \rightarrow \Lambda$), and the former rate[7] is at least 2 orders of magnitude slower (298 K) than the overall water exchange rate. Under these conditions, it may be expected that the observed rate of water exchange will be optimized for systems in which the twisted square-antiprismatic isomer predominates. Accordingly, we have studied in detail the structure and exchange dynamics of the complexes of the central lanthanide ions (Eu, Gd, Tb) with the four stereoisomers of 1,4,7,10-tetrakis(carboxyethyl)-1,4,7,10-tetraazacyclododecane, **4**, in the expectation that the isomeric composition (and hence water exchange rate) would vary between the lanthanide complexes of each ligand stereoisomer. Ligand **4** may exist as six different stereoisomers, determined by the configuration at each of the stereogenic centers at carbon: *RRRR*(*SSSS*); *RSSS*(*SRRR*) and the achiral diastereoisomers *RSRS* and *RRSS*. In the lanthanide complexes of a given octadentate ligand isomer, there are two further independent elements of chirality to consider, associated with the sign of the torsion angles of the NCCN chelate rings (λ or δ) and the NCCO chelates (defining the Δ or Λ) helicity of the N-substituents). Prior work with related ligands has established that, for a given isomer in solution, each chelate usually adopts the same configuration[8] so that four stereoisomers occur, which may interconvert by concerted ring inversions ($\delta\delta\delta\delta \rightarrow \lambda\lambda\lambda\lambda$) or cooperative arm rotation ($\Delta \rightarrow \Lambda$). Thus, for the lanthanide complexes of (*RRRR*)-**4**, for example, two pairs of square-

(7) (a) Hoeft, S.; Roth, K. *Chem. Ber.* **1993**, *126*, 869. (b) Aime, S.; Botta, M.; Ermondi, G. *Inorg. Chem.* **1992**, *31*, 4291. (c) Jacques, V.; Desreux, J. F. *Inorg. Chem.* **1994**, *33*, 4048.

Scheme 2

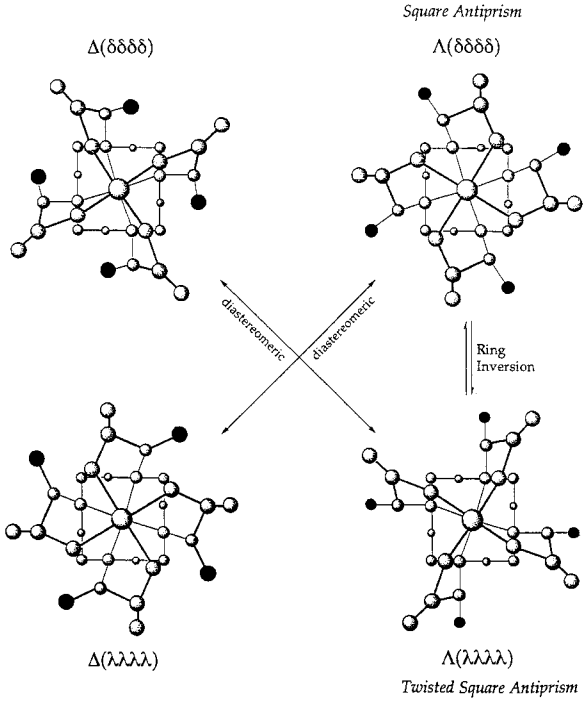

antiprismatic (twist angle ~40°) and twisted square-antiprismatic isomers (twist angle 29°) may exist (Scheme 2). Aspects of part of this work have been reported in a preliminary communication.[9]

Results and Discussion

Alkylation of 1,4,7,10-tetraazacyclododecane with racemic dimethyl-α-bromo glutarate (K_2CO_3/MeCN) led to formation of the octamethyl ester, as a mixture of diastereoisomers. Base hydrolysis (NaOH/MeOH−H_2O/70 °C, 18 h) yielded a mixture of the corresponding acids which was analyzed by reverse-phase HPLC. In the absence of any diastereoselectivity, this sequence should statistically yield 50% of the *RRRS*/*SSSR* pair, 25% of the *RRSS*, and 12.5% of the *RRRR*/*SSSS* and *RSRS*. Analysis by HPLC revealed three main peaks in ratio 3:1:1, the larger of which resolved into two peaks (~5:1) under gradient-eluting conditions which favored longer retention. Fractional crystallization of the mixture from dilute aqueous acid (pH 3) afforded the separate isomers whose configuration was established by NMR and crystallographic methods. The C_4 symmetric racemate was the least soluble stereoisomer and was easily differentiated by ^{1}H and ^{13}C NMR as the solution spectra were the least complex, giving, for example, six ^{13}C resonances (pD 6, 293 K). The relative configuration of each of the other three isomers was assigned by X-ray crystallographic (Figure 1) analyses on recrystallized samples of the separated isomers, grown from acidic aqueous or acidic aqueous ethanolic media, (see the Supporting Information for details). The structures of the (*RRRS*)/(*SSSR*) and (*RSRS*) isomers revealed that the 12-membered macrocyclic ring adopted the

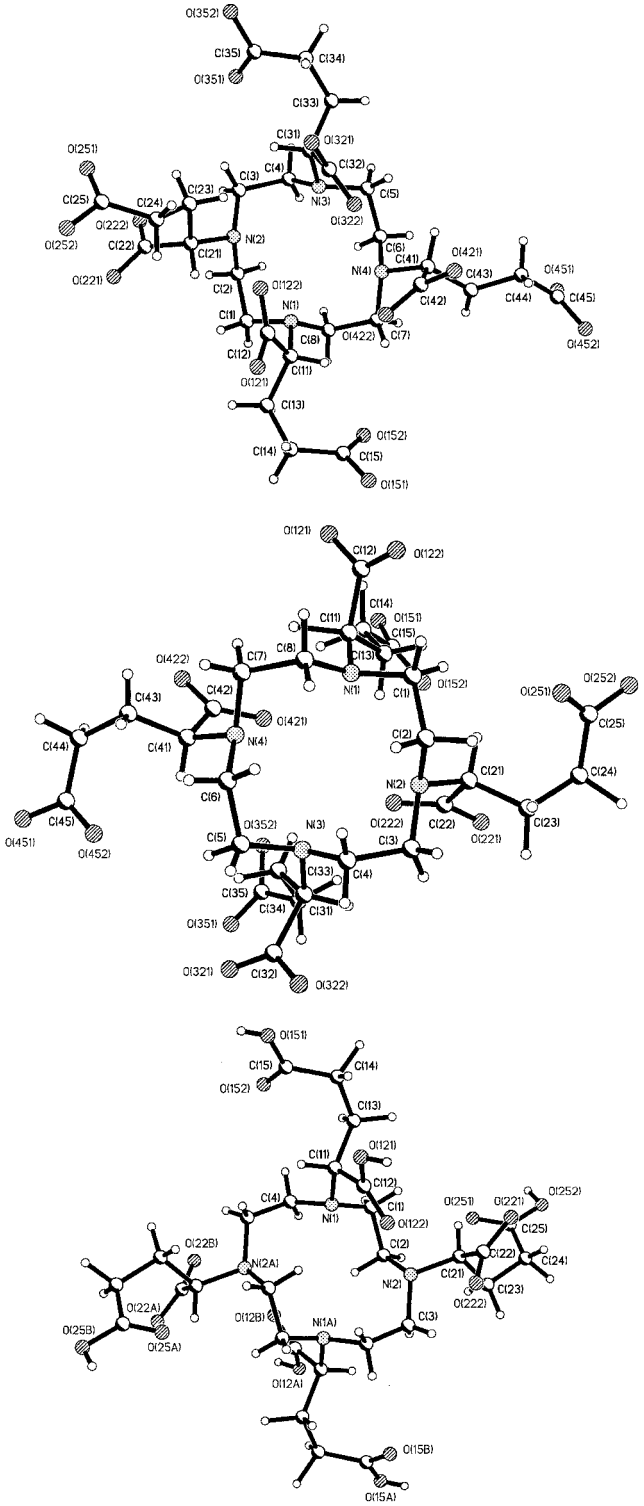

Figure 1. Crystal structures of (*RRRS*)-**4** (top), (*RSRS*)-**4** (center) and (*RRSS*)-**4** (bottom) determined at 150 K.

square [3333] conformation,[10] which is often found in lanthanide complex structures[8,11] and in the ligand dota itself.[6d] In the *RRSS* ligand stereoisomer (Figure 1), the ring conformation is slightly distorted with pairs of ring nitrogens and N-substituents related by the inversion center. The *RSRS* isomer closely resembles that reported recently for dota itself,[6d] with hydrogen bonding between each protonated ring N and the carbonyl group of the proximate CO_2H moiety.

(8) (a) Amin, S.; Morrow, J. R.; Lake, C. H.; Churchill, M. R. *Angew. Chem., Int. Ed. Engl.* **1994**, *33*, 773. (b) Dickins, R. S.; Howard, J. A. K.; Lehmann, C. W.; Moloney, J. M.; Parker, D.; Peacock, R. D. *Angew. Chem., Int. Ed. Engl.* **1997**, 521. (c) Dickins, R. S.; Howard, J. A. K.; Maupin, C. L.; Moloney, J. M.; Parker, D.; Peacock, R. D.; Riehl, J. P.; Siligardi, G. *New. J. Chem.* **1998**, 891. (d) Aime, S.; Barge, A.; Botta, M.; Howard, J. A. K.; Kataky, R.; Lowe, M. P., Moloney, J. M., Parker, D., de Sousa, A. S. *Chem. Commun.* **1999**, 1047.

(9) Woods, M.; Howard, J. A. K.; Kenwright, A. M.; Moloney, J. M.; Navet, M.; Parker, D.; Port, M.; Rousseau, O. *Chem. Commun*. **1998**, 1381.

(10) (a) Dale, J. *Top. Stereochem.* **1976**, *9*, 199. (b) Dale, J. *Isr. J. Chem.* **1980**, *87*, 1076.

Table 1. Crystal Data and Structure Refinement Details[a] for H_3O^+ [LnH_4 **1**.OH_2]$^-$2H_2O (Ln = Eu, Gd, Tb)[a]

	Ln		
	Eu	Gd	Tb
empirical formula	$C_{28}H_{49}O_{20}Eu$	$C_{28}H_{49}N_4O_{20}Gd$	$C_{28}H_{49}N_4O_{20}Tb$
formula weight	917.67	918.96	920.63
temperature (K)	150(2)	150(2)	150(2)
crystal size (mm)	0.16 × 0.16 × 010	0.34 × 0.32 × 0.18	0.10 × 0.20 × 0.25
crystal system	triclinic	triclinic	triclinic
space group	*P*-1̄	*P*-1̄	*P*-1̄
unit cell, dimens			
a (Å)	9.637(2)	9.6460(5)	9.6289(1)
b (Å)	12.690(4)	12.6915(7)	12.6877(2)
c (Å)	16.186(5)	16.2000(11)	16.2170(2)
α (deg)	102.47(2)	102.652(4)	102.739(1)
β (deg)	101.28(2)	101.192(4)	101.235(1)
γ (deg)	110.42(2)	110.446(3)	110.581(1)
volume, *Z* (Å^3/2)	1729.84(3)	1731.9(2)	1726.76(4)
$D_{calcd.}$ (g/cm^3)	1.762	1.762	1.762
radiation	Mo Kα	Mo Kα	Mo Kα
absorptn coeff (mm^{-1})	1.906	2.007	2.141
F(OOO)	940	938	940
θ range for data collection (deg)	1.35−27.45	1.35−27.50	1.35−27.53
no. of reflctns measd	13 944	14 872	13 969
no. of independent reflctns	7826	7843	7856
data/restraints/params	7797/0/624	7843/0/651	7856/0/10
goodness of fit on F^2	1.094	1.046	1.085
final *R* indices [$I > 2\sigma(I)$]	R_1 0.030, wR_2 0.067	R_1 0.021, wR_2 0.051	R_1 0.044, wR_2 0.106
largest diff peak and hole (e Å^{-3})	0.979/−0.950	0.656/−0.724	2.683/−2.362

[a] Data were collected on a Siemens Smart instrument. Refinement was by full-matrix, least squares on F^2 (SHELX 93). Data for the Eu complex have been deposited earlier (CCDC 182/875).

Structures of the Eu, Gd, and Tb Complexes of (*RRRR*)-4. Crystals of the europium, gadolinium, and terbium complexes of (*SSSS*)/(*RRRR*)-**4** were grown from dilute aqueous acidic media. The crystal structures were determined at 150 K (Figure 2) and revealed an isostructural series crystallizing in the *P*-1̄ space group (Tables 1 and 2). The geometry about the lanthanide ion was a monocapped square-antiprism with a twist angle (N_4/O_4 planes) averaging 38.5°. Thus, for an *R* configuration at carbon, the complex adopted a Λ helicity and the five-ring NCCN chelates were all *δ* (viz. Scheme 2). The (*SSSS*) enantiomer accordingly gave a Δ (right-handed) helicity, with a *λ* configuration in each of the five-ring NCCN chelate rings. Thus for (*RRRR*)-[Gd·**4**], the mean NCCN torsion angle was −59.5° and the NCCO angle averaged +34.6°. The mean Ln−N and Ln−O bond distances revealed the expected reduction in distance between lanthanides, consistent with the small ionic radius change from Eu to Tb (Table 2). The Ln−OH_2 distances decreased only marginally, from 2.447(3) Å in the europium complex to 2.427(3) Å for terbium. Similar bond distances and stereochemical relationships have been defined in previous crystallographic studies of the complexes of dota[11] and related tetraamide ligands.[8]

NMR Solution Studies. Proton NMR spectra for the europium complex of each of the isomers of **4** were obtained (400 MHz, 293 K; Figure 3). Inspection of the complexity of the spectra obtained allows information to be gathered about the number of stereoisomers present in solution and their time-averaged symmetry. Previous studies with [Ln(dota)]$^-$ and [Ln·**1**]$^{3+}$ have demonstrated that two major diastereoisomers are present in solution,[6d,7] whose relative proportion is a function of the lanthanide ion, temperature, and solvent. These two isomers—a regular (monocapped) square-antiprismatic structure (M) and the twisted square-antiprismatic isomer (m) (Scheme 2)—are characterized by different dipolar shifts, with complexes of the former series often possessing the bigger paramagnetic shifts, for a given resonance. A particularly useful resonance to observe, for this purpose, is the most shifted axial ring proton. This resonates at ∼30−50 ppm and at ∼150−160 ppm for square-antiprismatic Eu and Yb complexes of tetracarboxylate-

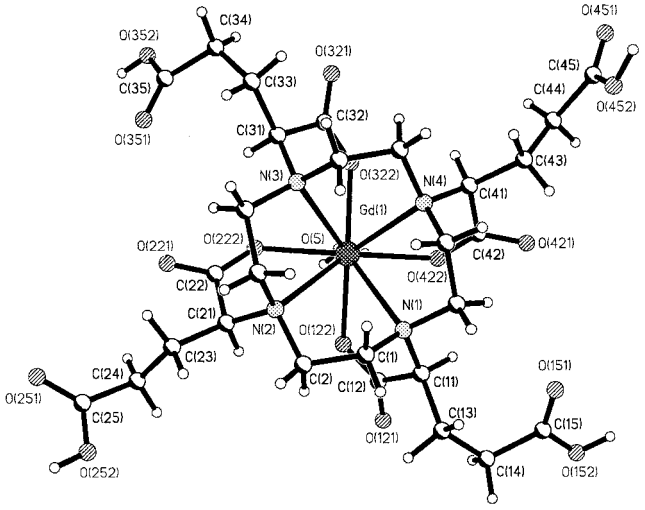

Figure 2. View of the crystal structure of H_3O^+ [(*SSSS*)-H_4 **4** (OH_2)Gd]$^-$·2H_2O determined at 150 K, highlighting the Δ/*λλλλ* configuration and the monocapped square-antiprismatic coordination geometry.

(11) See, inter alia: (a) Amin, S.; Voss, D. A.; Horrocks, W. de W.; Lake, C. H.; Churchill, M. R.; Morrow, J. R. *Inorg. Chem.* **1995**, *34*, 3294. (b) Kumar, K.; Chang, C. A.; Francesconi, L. C.; Dischino, D. D.; Malley, M. F.; Gougoutas, Z.; Tweedle, M. F. *Inorg. Chem.* **1994**, *33*, 3567, in this case, [Gd-HPDO3A], two independent M and m isomers were characterized crystallographically and the m isomer had a water−Gd distance only 0.01 Å longer than the M. Examples of phosphinate complexes with an m structure and Ln−water distances that are ∼0.12 Å longer than the corresponding carboxylate complexes include the following: (c) Aime, S.; Batsanov, A. S.; Botta, M.; Dickins, R. S.; Faulkner, S.; Foster, C. E.; Harrison, A.; Howard, J. A. K.; Moloney, J. M.; Norman, T. J.; Parker, D.; Royle, L.; Williams, J. A. G. *J. Chem. Soc., Dalton Trans.* **1997**, 3623. (d) Rohovec, J.; Vojtisek, P.; Hermann, P.; Mosinger, J.; Zak, Z.; Lukes, I. *J. Chem. Soc., Dalton Trans.* **1999**, 3585. (e) Rohovec, J.; Vojtisek, P.; Hermann, P.; Ludvik, J.; Lukes, I. *J. Chem. Soc., Dalton Trans*. **2000**, 141.

Table 2. Selected Bond Distances (Å) and Angles[a] (deg) for $H_3O^+[Ln{\cdot}H_4$ **1** $(OH_2)]^-{\cdot}2H_2O$

	Ln		
	Eu	Gd	Tb
Ln−O(5)[b]	2.447(3)	2.432(2)	2.427(4)
Ln−O(122)	2.393(2)	2.385(2)	2.368(4)
Ln−O(222)	2.354(2)	2.383(2)	2.371(3)
Ln−O(322)	2.412(2)	2.349(2)	2.335(3)
Ln−O(422)	2.391(2)	2.403(2)	2.386(4)
Ln−N(1)	2.681(3)	2.662(2)	2.654(4)
Ln−N(2)	2.696(3)	2.674(2)	2.665(4)
Ln−N(3)	2.664(3)	2.689(2)	2.686(4)
Ln−N(4)	2.667(3)	2.655(2)	2.644(4)
N(1)−C(1)−C(2)−N(2)	59.52(40)	−61.45(24)	−61.1(6)
N(2)−C(3)−C(4)−N(3)	58.43(36)	−59.59(26)	−58.7(6)
N(3)−C(5)−C(6)−N(4)	58.67(36)	−58.06(23)	−59.0(6)
N(4)−C(7)−C(8)−N(1)	60.86(37)	−58.94(23)	−58.1(6)
N(1)−C(11)−C(12)−O(122)	−38.52(50)	17.49(26)	18.2(6)
N(2)−C(21)−C(22)−O(222)	−39.69(38)	37.58(33)	38.1(8)
N(3)−C(31)−C(32)−O(322)	−40.62(38)	39.45(24)	39.2(6)
N(4)−C(41)−C(42)−O(422)	−17.50(40)	40.61(24)	40.6(6)
O(222)−Ln−O(122)	84.31(8)	85.82(6)	85.38(13)
O(122)−Ln−O(322)	144.73(8)	144.86(5)	144.33(12)
N(1)−Eu−N(2)	67.98(9)	69.56(5)	69.57(12)
O(122)−Eu−N(2)	73.13(9)	74.17(6)	74.10(13)
O(122)−Eu−N(1)	65.34(8)	65.28(5)	65.54(12)
O(5)−Eu−N(1)	125.29(10)	128.11(6)	127.81(15)

[a] Torsion angles are given for the (*RRRR*) isomer for Eu and the (*SSSS*) isomer for Gd and Tb. [b] Mean distances from Ln to the bound water protons were 2.85 (Eu), 2.84 (Gd), and 2.83 Å (Tb); the water hydrogens were located from the difference Fourier maps.

1,4,7,10-tetraazocyclododecane derivatives[7,8] at ambient temperature in D_2O. On the other hand, in the corresponding twisted square-antiprismatic isomers, the same ring axial proton resonates at about 20 and 60 ppm to lower frequency for Eu and Yb, respectively.[11c,7]

Two major isomeric species were observed for the (*RRRR*)-, (*RRRS*)-, and (*RSRS*)-[Eu·**4**] complexes, in a relative ratio, M/m of 1:4, 2:1, and 4:1, respectively. For (*RRSS*)-[Eu·**4**], only one (M) isomer was observed in solution. Two-dimensional $^1H-^1H$ COSY NMR experiments confirmed that only two species were present and allowed the assignments of most of the resonances to be made. For the (*RRRR*)-Eu complex,[12] the major (m) isomer must adopt a $\Lambda/(\lambda\lambda\lambda\lambda)$ configuration, while the minor (M) isomer possesses a $\Lambda/(\delta\delta\delta\delta)$ configuration. The absolute configuration of the stereogenic center at C is determining the left-handed helicity of the complex, so that neither the $\Delta/(\delta\delta\delta\delta)$ nor the $\Delta/(\lambda\lambda\lambda\lambda)$ complexes are present to any significant extent. In the case of (*RRSS*)- and (*RSRS*)-[Eu·**4**], the presence of the chiral centers does not change the stereoisomeric relationships found in complexes of the achiral ligand (dota), i.e., two enantiomeric sets of m and M isomers. Indeed, the form and shifts observed for (*RSRS*)-[Eu·**4**]$^{5-}$ are very similar to those found for $[Eu(dota)]^-$.[7,11] In the case of (*RRSS*)-[Eu·**4**]$^{5-}$, only the square-antiprismatic isomer was observed.

Exchange between the m and M isomers has been shown to occur by independent or concerted arm rotation or ring inversion (Scheme 2). These motions exchange the positions of protons within the complex: thus, the axial proton of the (M) isomer is exchanged with both the ring equatorial and axial protons of the minor (m) isomer by ring flip or arm rotation, respectively (Scheme 3). Sequential or concerted arm rotation and ring flip

(12) An (*RRRR*) configuration is arbitrarily specified here: for the (*SSSS*) enantiomer the same arguments apply, giving rise to the corresponding enantiomeric (m) and (M) complexes, which are indistinguishable in solution by NMR, in the absence of an external chiral influence.

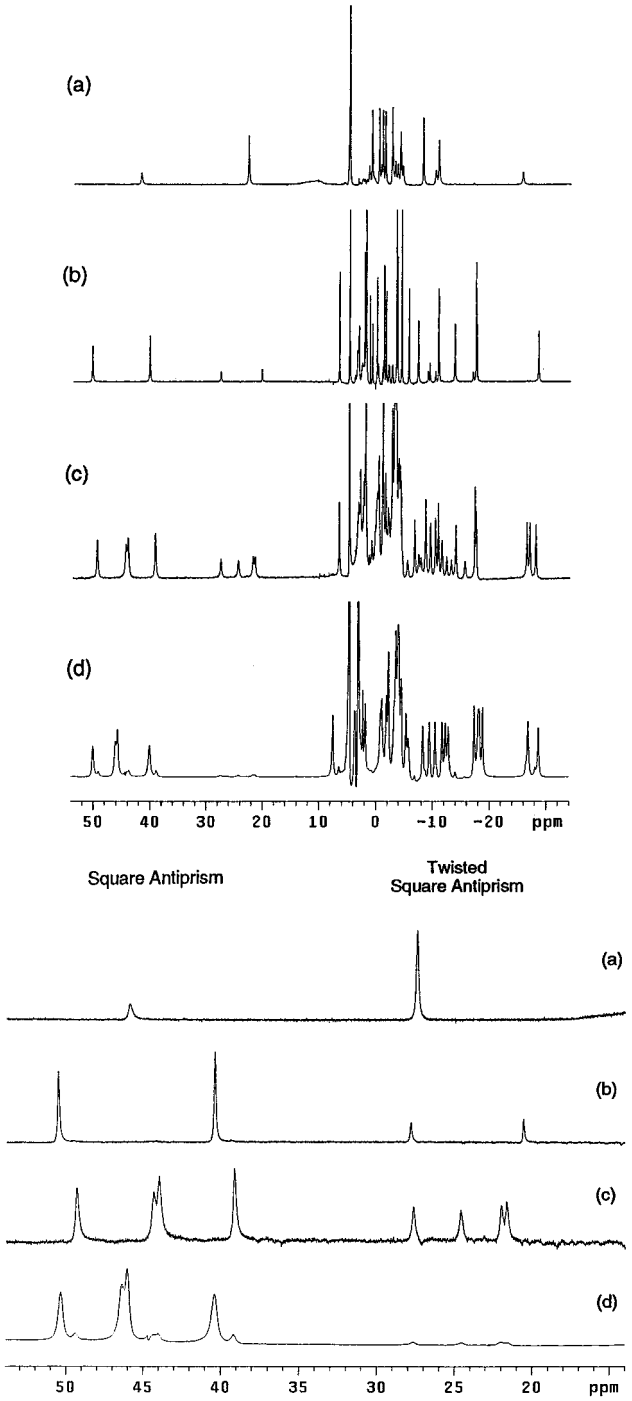

Figure 3. Proton NMR spectra (400 MHz, 293 K) of the (m) and (M) diastereoisomers of (a) (*RRRR*)-[Eu·**4**], (b) (*RSRS*)-[Eu·**4**], (c) (*RRRS*)-[Eu·**4**], and (d) (*RRSS*)-[Eu·**4**] showing the full spectra (upper) and the most shifted axial ring resonance (lower). The latter sample contained ~12% of the (*RRRS*) isomer, as an impurity.

allows exchange between $\Delta(\lambda\lambda\lambda\lambda)$ and $\Lambda(\delta\delta\delta\delta)$ diasteroisomeric (M) pairs. Two-dimensional EXSY spectra were recorded at 400 MHz and 293 K for the europium complexes of (*RRRR*)-, (*RRRS*)-, and (*RSRS*)-**4**. The nature and form of the EXSY spectrum for the (*RSRS*)-[Eu·**4**]$^{5-}$ complex was very similar to that reported for $[Eu(dota)]^-$.[7a] Thus, the pair of axial proton resonances at 50.3 and 40.1 ppm due to the major (M) isomer showed cross-peaks with both the axial and equatorial protons of the minor, twisted square-antiprismatic isomer. Such behavior is consistent with relatively fast ring inversion and arm rotation on the NMR time scale at 293 K. The EXSY spectra obtained

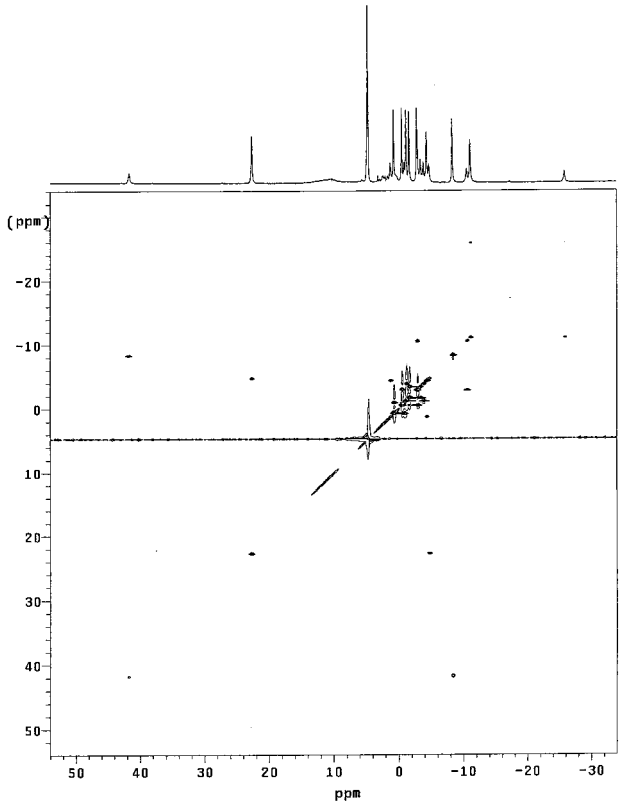

Figure 4. ^{1}H NMR EXSY spectrum (500 MHz) for (*RRRR*)-[Eu·**4**], showing the correlation between the ring axial protons in the m and M isomers (δ 22 and 41.9, respectively) and the ring equatorial protons at −4.9 and −8.6 ppm resulting from concerted ring inversion.

Scheme 3

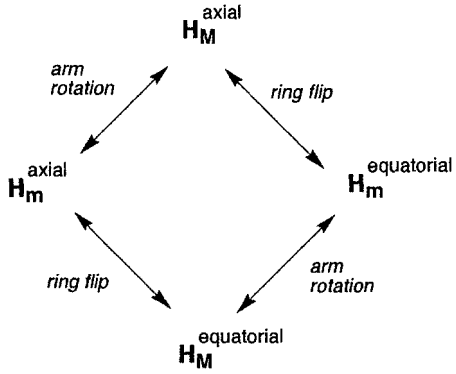

for (*RRRR*)-[Eu·**4**]$^{5-}$ and (*RRRS*)-[Eu·**4**]$^{5-}$ were much simpler: only one set of cross-peaks was evident in each case. For example, with (*RRRR*)-[Eu·**4**], there was a correlation between the axial proton at +22.0 ppm (major m isomer) and an equatorial ring proton in the minor square-antiprismatic (M) isomer, resonating at −4.9 ppm (Figure 4). Similarly, the axial ring proton resonance at +41.9 ppm (minor M isomer), correlated with the ring equatorial proton resonance at −8.6 ppm, attributed to the major (m) twisted square-antiprismatic complex. No cross-peaks were observed between corresponding axial proton resonances of the major and minor isomers, indicating that concerted arm rotation was occurring much more slowly under these conditions. Parallel behavior was observed for the *RRRS*-[Eu·**4**] complex, and in each case, further variable-temperature studies were carried out in an effort to estimate the barrier to arm rotation. Variable-temperature ^{1}H NMR spectra of the most shifted axial ring proton resonances for the (*RRRR*)- and (*RRRS*)-europium complexes were measured over the range 293−333 K, (Figure 5). No coalescence phenomenon was directly observed, and while each resonance did broaden at higher temperatures, the small variation in the separation between the pair (or sets) of peaks in each case, was at least partly attributable to the temperature dependence of the paramagnetic shift.

More precise rate information on the ring inversion process was obtained using saturation transfer methods,[13] monitoring exchange between the axial ring proton resonance at +41.9 ppm in (*RRRR*)-[Eu·**4**] and the equatorial ring proton resonance at −8.6 ppm. The rate of inverconversion of the M → m isomers was estimated to be 45 (±15) s^{-1} at 293 K, similar to the value of 35 s^{-1} measured for ring inversion in [Eu(dota)]$^-$ at room temperature.[7a] For the (*RRRS*)-[Eu·**4**] complex, the ring inversion rate was estimated to be 40 (±15) s^{-1}. It is clear that the motion of cooperative ring inversion, exchanging m and M isomers, occurs independently of arm rotation and at a rate that may be conservatively estimated to be at least 2 orders of magnitude faster at 293 K. The introduction of substituents α to the ring N, on the dota ligand, has previously been shown to inhibit arm rotation,[14a] and similar inhibition of this motion occurs with the lanthanide complexes of the chiral tetraamides[14b] [Ln·**3**]$^{3+}$ and the related series of tetraalkylphosphinoxymethyl derivatives of cyclen,[15] which introduce a stereogenic center γ or β to the ring nitrogen, respectively.

The ratio of diastereoisomers in solution also varies as a function of the lanthanide ion. For the (*RRRR*) isomer, the ratio of the twisted (m) to the regular (M) square-antiprismatic complex was measured by ^{1}H NMR integration of the shifted axial ring resonances for six different lanthanide ions. In each case, the (m) isomer predominated in solution (293 K) with values of 20:1 (Pr), 8:1 (Nd), 4:1 (Eu), 1.5:1(Tb), 4:1 (Ho), and 15:1 (Yb). The form of the variation of the m/M ratio is rather different from that observed with [Ln(dota)]$^-$ complexes: in that case, the square-antiprismatic isomer dominates, with the M/m ratio being very large for Ce and Pr, reaching a maximum around Ho/Er, before falling again at the end of the lanthanide series.[7a,b,16]

Luminescence Studies of Eu and Tb Complexes. Emission spectra for the Eu complexes of each stereoisomer were recorded under moderate resolution following direct excitation of the Eu ion at 393 nm (293 K, D_2O). The form of the emission spectra in the range 575−710 nm for the (*RRRS*), (*RSRS*), and (*RRSS*) isomers was very similar, with little change in the relative intensity of the $\Delta J = 1$ transitions (two major components at ∼590 nm) and the hypersensitive $\Delta J = 2$ manifold at ∼618 nm. Indeed, the emission spectra closely resembled that of [Eu(dota)]$^-$, consistent with a similar local coordination environment (i.e., major square-antiprismatic, nine-coordinate; N_4O_5 donor set). The spectrum of the (*RRRR*)-[Eu·**4**] complex was notably different in the $\Delta J = 1$ and $\Delta J = 4$ bands. The magnetic dipole-allowed transition, $^5D_0 - ^7F_1$, generally possesses an intensity that changes little from one coordination environment to another; three transitions are allowed in low symmetry but only two if the complex possesses a C_3 or C_4 axis. The magnitude of the separation of the two peaks in such axially

(13) Sanders, J. K. M.; Hunter, B. K. *Modern NMR Spectroscopy*; OUP: Oxford, 1988; p 224.

(14) (a) Aime, S.; Botta, M.; Ermondi, G.; Terreno, E.; Anelli, P. L.; Uggeri, F. *Inorg. Chem.* **1996**, *35*, 2726. (b) Dickins, R. S.; Howard, J. A. K.; Maupin, C. L.; Moloney, J. M.; Parker, D.; Siligardi, G.; Williams, J. A. G. *Chem. Eur. J.* **1999**, *5*, 1095.

(15) Aime, S.; Botta, M.; Parker, D.; Senanayake, K.; Williams, J. A. G.; Batsanov, A. S.; Howard, J. A. K. *Inorg. Chem.* **1994**, *33*, 4696.

(16) Aime, S.; Botta, M.; Fasano, M.; Marques, M. P. M.; Geraldes, C. F. G. C.; Pubanz, D.; Merbach, A. E. *Inorg. Chem.* **1997**, *36*, 2059.

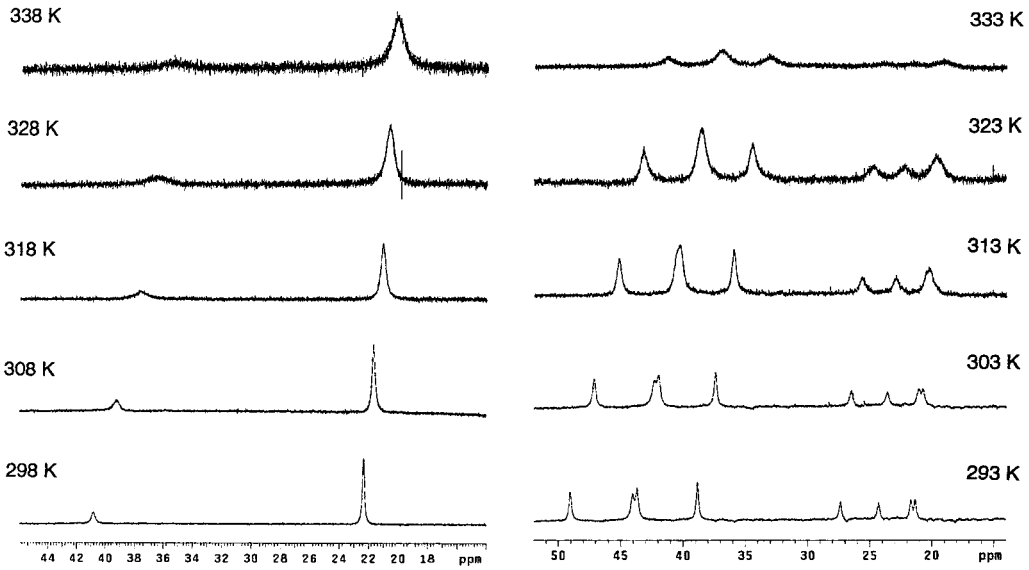

Figure 5. Variable-temperature ^{1}H NMR (400 MHz) spectra for (*RRRR*)-[Eu·**4**] (left) and (*RRRS*)-[Eu·**4**] (right), showing the most shifted axial ring proton resonance.

symmetric complexes is directly proportional to the size of the dipolar NMR shift, as both are determined by the crystal field coefficient A^o_2.[27] For [Eudota]$^-$, there are two major bands in this region (Figure 6) and the weaker central band relates to the presence of the minor (m) isomer. In (*RRRR*)-[Eu·4], the m/M ratio is 4:1 and the central transition increases in intensity accordingly. Profound changes in the form and relative intensity of the hypersensitive $\Delta J = 4$ manifold also characterize the differences between the m and M isomeric complexes.

Rate constants for depopulation of the excited states of each of the Eu and Tb isomeric complexes were measured in H_2O and D_2O at 293 K, allowing the degree of hydration of the complexes to be estimated. Recently, an improvement[17] to the original method[18] of analysis has been promulgated, wherein the quenching effect of closely diffusing (i.e., unbound) OH oscillators on the Eu ^5D_o or Tb $^5D_4$ excited state is accounted for, rather than disappearing as a term inherent in the estimated error. Values obtained for the hydration state, q (Table 3), showed that the Eu complexes possessed values of $q = 1$ (within the experimental error), as did the (*RRSS*)- and (*RSRS*)-[Tb·**4**]

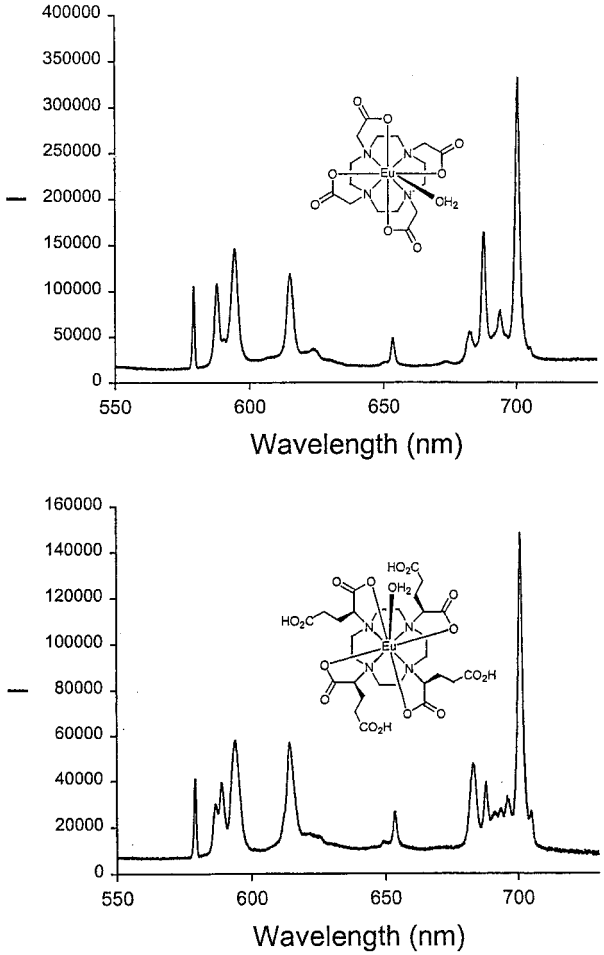

Figure 6. Metal-based luminescence emission spectra for [Eudota]$^-$ (4:1 ratio of M/m isomers) and of (*RRRR*)-[Eu·**4**] (1:4 ratio of M/m isomers) highlighting the differences in the $\Delta J = 1$ (590 nm) and $\Delta J = 4$ (700 nm) transitions.

(17) Beeby, A.; Clarkson, I. M.; Dickins, R. S.; Faulkner, S.; Parker, D.; Royle, L.; de Sousa, A. S.; Williams, J. A. G.; Woods, M. *J. Chem. Soc., Perkin Trans. 2*, **1999**, 493.

(18) Horrocks, W. de W.; Sudnick, D. R. *Acc. Chem. Res*. **1981**, *14*, 384.

(19) Aime, S.; Botta, M.; Parker, D.; Williams, J. A. G. *J. Chem. Soc., Dalton Trans*. **1996**, 17.

(20) Aime, S.; Botta, M.; Dickins, R. S.; Maupin, C. L.; Parker, D.; Riehl, J. P.; Williams, J. A. G. *J. Chem. Soc., Dalton Trans.* **1998**, 881.

(21) Spirlet, M.-F.; Rebizant, J.; Wang, X.; Jin, T.; Gilsoul, D.; Comblin, V.; Maton, F.; Muller, R. N.; Desreux, J. F. *J. Chem. Soc., Dalton Trans*. **1997**, 497. For [GdODOTRA], an m isomeric structure was defined with a water−Gd bond distance that was ∼0.1 Å longer than expected, if a correlation with the corresponding bond length in related M complexes is considered valid.

(22) Swift, T. J.; Connick, R. E. *J. Chem. Phys*. **1962**, *37*, 307; **1964**, *41*, 2553. See also: Aime, S.; Botta, M.; Fasano, M.; Paoletti, S.; Terreno, E. *Chem. Eur. J*. **1997**, *3*, 1499.

(23) The assumption that $q = 1$ in each case is supported by the luminescence studies and by the characteristic inflection in the profile, observed in each case, in the region 5−10 MHz.[1]

(24) The low-field region of the NMRD profile is primarily determined by τ_{SO}—the electron-spin relaxation time at zero field. Inspection of Table 4 and Figure 7 and comparison to the established τ_{SO} values for [Gd(dota)]$^-$ suggest that τ_{SO} cannot be solely influenced by the local symmetry at the metal center but may also be dependent upon the degree of rigidity at the metal center, especially associated with changes in local helicity due to arm rotation.

(25) Dunand, F.; Aime, S.; Merbach, A. E. *J. Am. Chem. Soc*. **2000**, *122*, 1506

(26) Sheldrick, G. M. SHELXL-93, University of Gottingen, Gottingen, 1993.

(27) Judd, B. R. *Mol. Phys*. **1959**, *2*, 407. Bleaney, B. *J. Magn. Reson*. **1972**, *8*, 91. Golding, R. M.; Pyykko, P. *Mol. Phys*. **1973**, *26*, 1389.

Table 3. Rate Constants (ms^{-1}) for Depopulation of the Excited States of Eu[a] and Tb[b] Complexes in H_2O and D_2O (293 K; ±7%)

complex	k_{H_2O}	k_{D_2O}	Δk	Δk_{corr}	q_{corr}[c]
[Eu(*RRRR*)-**1**]$^{5-}$	1.61	0.48	1.13	0.88	1.06
[Eu(*RRRS*)-**1**]$^{5-}$	1.49	0.40	1.09	0.84	1.01
[Eu(*RRSS*)-**1**]$^{5-}$	1.50	0.48	1.02	0.77	0.92
[Eu(*RSRS*)-**1**]$^{5-}$	1.54	0.44	1.10	0.85	1.02
[Tb(*RRRR*)-**1**]$^{5-}$	0.48	0.30	0.18	0.12	0.60
[Tb(*RRRS*)-**1**]$^{5-}$	0.52	0.31	0.21	0.15	0.75
[Tb(*RRSS*)-**1**]$^{5-}$	0.56	0.30	0.26	0.20	1.00
[Tb(*RSRS*)-**1**]$^{5-}$	0.55	0.30	0.25	0.19	0.95
[Eu(dota)]$^{-}$	1.60	0.53	1.07	0.82	0.98
[Tb(dota)]$^{-}$	0.66	0.39	0.27	0.21	1.05

[a] Values of Δk_{corr} were obtained by subtracting 0.25 ms^{-1}, to allow for the quenching effect of closely diffusing (unbound) OH oscillators: see ref 17 for a full discussion. [b] Δk values were corrected by −0.06 ms^{-1} to give Δk_{corr}. [c] $q_{corr}^{Eu} = 1.2\ \Delta k_{corr}$ and $q_{corr}^{Tb} = 5\ \Delta k_{corr}$.

complexes. The hydration state of the (*RRRR*)- and (*RRRS*)-Tb complexes gave q values of 0.60 and 0.75, apparently below an integral value. Nonintegral values of q have been observed previously for related complexes[17,19] and may be ascribed to a mixture of $q = 0$ and $q = 1$ complexes[16] (i.e., 8/9 coordinate complexes), to the presence of a significant second-sphere of hydration,[20] or to the occurrence of a species with an elongated Ln−OH_2 bond.[17] In the latter case, as a consequence of the $1/r^6$ relationship for the efficiency of vibrational energy transfer, the elongation of the Ln−OH_2 bond by 0.12 Å may be calculated to cause a reduction in the effective q value by 20%.[17] Given that the reported values of elongated Ln−OH_2 bonds all occur in monocapped twisted square-antiprismatic complex structures,[11c,21] then it is plausible that there is a correlation between the nonintegral Tb q values and the proportion of the twisted square-antiprismatic isomer found for the (*RRRR*) and (*RRRS*) isomeric complexes. Further work is required, however, to substantiate this argument.

Relaxometric and ^{17}O NMR Study of the Gadolinium Complexes. An NMRD study was undertaken in aqueous solution at pH 6 in the presence of the isomeric (*RRRR*)-, (*RRRS*)-, and (*RSRS*)-[Gd·**4**] complexes. The profiles were recorded on the Koenig−Brown field-cycling relaxometer at 288, 298, and 312 K in the proton Larmor frequency range of 0.01−50 MHz. In the high-field region, the relaxivity is very similar for the three isomers (Figure 7), as expected since (i) the relaxivity of small gadolinium chelates at high fields depends primarily upon the rotational correlation time τ_R and (ii) their identical molecular mass, dimension, and charge results in a strictly similar rotational dynamics. In the low-field region, r_{1p} is frequency independent and differs among the three complexes as a result of the different values for the electronic relaxation times,[24] as previously observed for other isomeric dota-like complexes.[6e] The experimental profiles were fitted to the equations for inner- and outer-sphere paramagnetic relaxation (see Supporting Information) to give the parameters listed in Table 4. In the analysis, the value of τ_R/r^6 at each temperature was set equal for the three complexes and a reasonable choice was made for r (2.92 Å), based on estimates from crystallographic data (see Table 2, for example). The parameters a (3.8 Å) and D were fixed to typical values and $q = 1$ was assumed for the three complexes.[23] It must be noted that a variation of a of ±0.2 Å results only in a ±4% difference in τ_R. The profiles depend only slightly on the actual value of the water residence lifetime τ_M, which then cannot be determined with sufficient accuracy.

An independent assessment of this important parameter was obtained by a variable-temperature, proton-decoupled ^{17}O NMR measurement of the water nuclear transverse relaxation rate. Such a study gives information on the water oxygen exchange rate at the paramagnetic center, by fitting the observed profiles to the Swift−Connick equations, using a well-established procedure (Figure 8).[22] In the analysis, we used a standard value for the hyperfine coupling constant A/h (-3.8×10^6 rad s^{-1}) between the electron and nuclear spins and for the electron relaxation times (Δ^2 and τ_V) the values calculated by the NMRD profiles. From the experimental data, we obtained the values of the *apparent* water exchange rate k_{ex} ($k_{ex} = 1/\tau_M$), its temperature dependence (ΔH_M), and the temperature dependence of the electron relaxation rate (ΔH_V), as reported in Table 5.

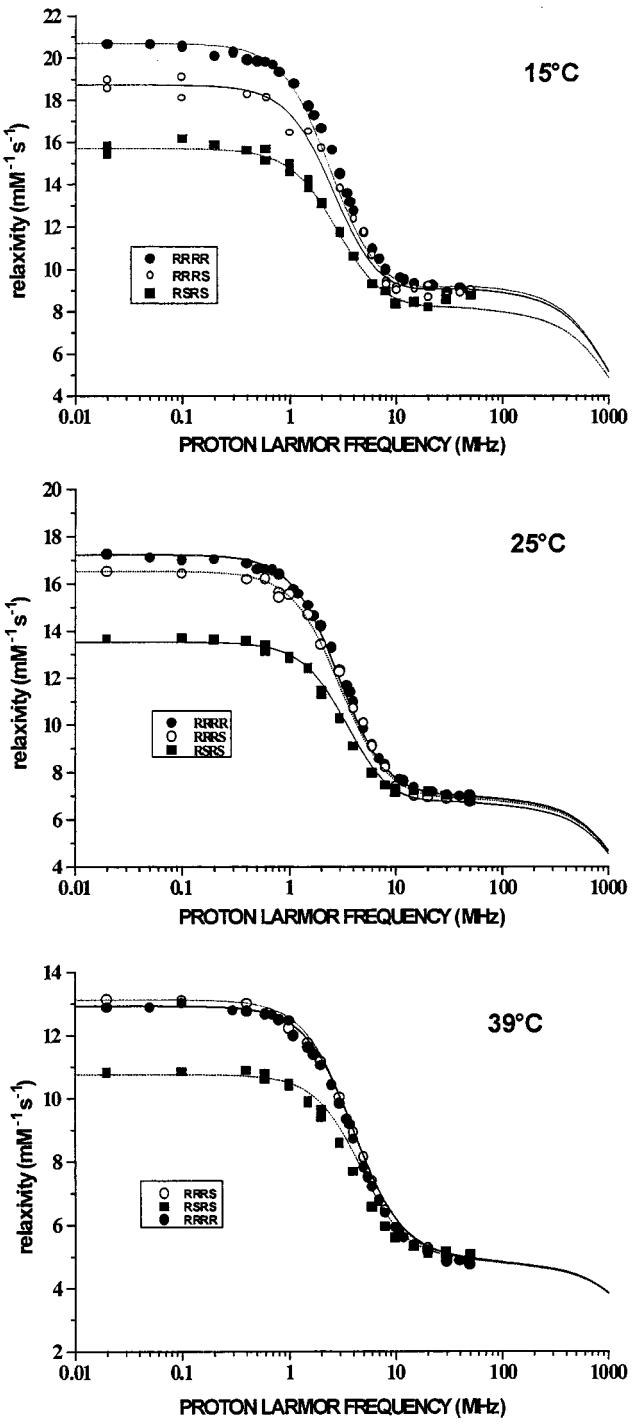

Figure 7. Comparison of the NMRD profiles for (*RRRR*)-[Gd·**4**] and the (*RRRS*) and (*RSRS*) isomeric complexes at 288, 298, and 312 K. The continuous and dotted lines show the fits to the experimental data.

Table 4. Best Fitting Parameters Determined by Analyses of NMRD Profiles for Isomeric Gadolinium Complexes[a]

	[(*RRRR*)-Gd·**4**]$^-$			[(*RRRS*)-Gd·**4**]$^-$			[(*RSRS*)-Gd·**4**]$^-$		
parameter	15 °C	25 °C	39 °C	15 °C	25 °C	39 °C	15 °C	25 °C	39 °C
$\Delta^2(s^{-2} \times 10^{19})$	1.9 ± 4	2.3 ± 0.2	3.2 ± 0.2	1.9 ± 0.3	2.5 ± 0.3	3.8 ± 0.3	1.9 ± 0.6	3.2 ± 0.3	4.4 ± 0.3
τ_v (ps)	12 ± 3	10 ± 2	8 ± 1	15 ± 2	10 ± 2	6 ± 1	16 ± 2	14 ± 2	12 ± 1
τ_r ps)	159 ± 4	116 ± 2	77 ± 2	159 ± 3	116 ± 2	77 ± 2	159 ± 4	116 ± 2	77 ± 2
τ_m (ns)[b,c]	190 ± 7	68 ± 470	16 ± 3	260 ± 9	140 ± 5	30 ± 4	730 ± 14	270 ± 9	87 ± 5

[a] In each case, $q = 1$; $r = 2.92$ Å; a, the distance of the closest approach of diffusing water was set at 3.8 Å and the diffusion coefficient, D, was estimated to be 1.65, 2.40, and 3.15 $cm^2\ s^{-1}$ at 15, 25, and 39 °C, respectively. [b] The values refer to measurement of the water exchange rate obtained from variable-temperature ^{17}O NMR R_{2p} measurements. [c] For comparison, τ_m (298 K) values for [Gd.dota]$^-$ and (*RRRR*)-[Gd.dotma]$^-$ were measured to be 244 and 68 ns, respectively; for [Gd(dota)]$^-$ (298 K): $\tau_v = 7.2$ ps, $\tau_r = 73$ ps.

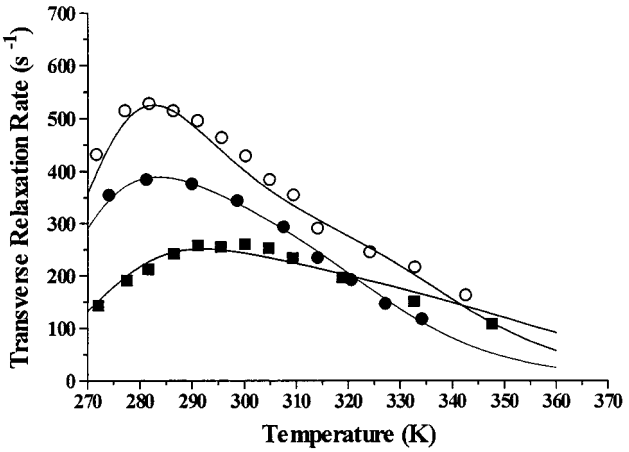

Figure 8. Temperature dependence of the ^{17}O NMR (12 MHz) transverse relaxation rates for (*RRRR*)-[Gd·**4**] (filled circles), (*RRRS*)-[Gd·**4**] (open circles), and (*RSRS*)-[Gd·**4**] (filled squares). The complex concentration was 50 mM in each case.

Table 5. ^{17}O NMR Best Fitting Parameters for Isomeric Gadolinium Complexes

	[(*RRRR*)-Gd·**4**]$^-$	[(*RRRS*)-Gd·**4**]$^-$	[(*RSRS*)-Gd·**4**]$^-$
k_{ex}^{298} ($\times 10^6\ s^{-1}$)	14.7 ± 1	7.1 ± 2	3.7 ± 1
ΔH_M (kJ/mol)	73 ± 4	66 ± 3	64 ± 4
ΔH_V (kJ/mol)	10 ± 1	26 ± 3	5 ± 0.7
ΔH_R[a] (kJ/mol)	20	20	20

[a] Fixed in the fitting.

Such an analysis is intrinsically limited in its accuracy, as the rates and activation energies for water exchange with the two isomeric species may differ significantly. Different values of k_{ex} and its temperature dependence were examined in a matrix of fitted minima, and the most chemically reasonable values were identified and are those given in Table 5. An estimated error of ±20% is associated with the k_{ex} values obtained by such an analysis. The values of the *apparent* water residence lifetime τ_M obtained from this procedure, at 298 K, are 68, 140, and 270 ns for the (*RRRR*), (*RRRS*), and (*RSRS*) isomeric complexes, respectively. For comparison, values measured for [Gd(dota)]$^-$ and [Gd(dotma)]$^-$ under the same conditions were 244 and 68 ns. These results highlight the higher water exchange rate associated with those complexes which possessed a higher proportion of the twisted square-antiprismatic isomer in solution (determined for the corresponding Eu and Tb complexes). It must be emphasized that the values of the water exchange obtained by this procedure represent only a crude estimation. This is a common limitation encountered in the relaxometric investigations of most of the Gd chelates. To a first approximation, the observed rate of water exchange, k_{ex}, is given by eq 3,

$$k_{ex} = P_M k_M + P_m k_m \quad (3)$$

where k_M, k_m and P_m, P_M are the separate rates of exchange and mole fractions for the m and M isomers, respectively, and K is their isomeric ratio (M/m), with $P_M = K/(K + 1)$ and $P_m = 1/(K + 1)$. Recently, in a study of related Eu−tetramide complexes, it was shown that the m isomer undergoes dissociative water exchange 50 times faster than the M isomer at 298K.[6d,25] Using the assumption that k_m/k_M is ∼50, then eq 3 may be rearranged and simplified to eq 4. Such an approximation allows the value of k_m to be measured for each complex, provided that the mole fraction P_m is known. These values were measured by ^1H NMR in solution for the corresponding Eu and Tb complexes and average values were derived therefrom (Table 6). Thus, values of k_m could be estimated for each complex and for the related complexes [Gd(dota)]$^-$ and [Gd(dotma)]$^-$. It is found that k_m is constant, i.e., independent of isomeric structure, and equal to $\sim 2.1 \times 10^7\ s^{-1}$ (or $\tau_M = 48$ ns at 298 K). Hence, the rate of water exchange at a Gd center is determined by the proportion of the m isomer present in solution, in agreement with the observations made on water exchange dynamics on related Eu−amide complexes.[6b,d,25]

$$k_m = k_{ex}/P_m \quad (4)$$

Table 6. Molar Fractions, Observed (k_{Ex}) and Calculated (k_m) Water Exchange Rates at 298 K for the Gd Complexes

complex	P_m[a]	k_{ex} (s^{-1})	k_m (s^{-1})
(*RRRR*)-[Gd·**4**]	0.7	1.54×10^7	2.2×10^7
(*RRRR*)-[GdDOTMA]	0.7	1.47×10^7	2.1×10^7
(*RRRS*)-[Gd·**4**]	0.43	9.0×10^6	2.1×10^7
[Gd·DOTA]	0.17	4.1×10^6	2.4×10^7
(*RSRS*)-[Gd·**4**]	0.17	3.45×10^6	2.0×10^7

[a] Average value for related Eu and Tb complexes.

The approach followed for the determination of the kinetic parameters of Table 6 is based on the assumption that eq 3 represents a good approximation. In principle, this is true only for the ^{17}O relaxation data in the low-temperature region where the R_2 data are proportional to k_{ex}. In general, since we have in solution a mixture of two isomers, the ^{17}O R_2 values will depend on the following: k_{ex} and its temperature dependence (ΔH_M), the electronic relaxation rate and its temperature dependence (Δ^2, τ_V, ΔH_V), and the hyperfine coupling constant for isomer M and the same six parameters for isomer m. Furthermore, we need to know at each temperature the isomeric distribution (ΔG^{isom}) and then 13 parameters are necessary to determine the temperature dependence of the ^{17}O relaxation rates. This may be possible if the k_{ex} values of the two isomers differ by several orders of magnitude; this is not the case here, as can be seen from the shape of the ^{17}O profiles. However, we can make several good approximations: for the structural (r, a) and electron relaxation parameters, the differences between the two isomers are probably negligeable ([Gd(dota)]$^-$ and [Gd(dotma)]$^-$ have nearly identical NMRD profiles) and ΔG^{isom} can be calculated from the proton NMR spectra of the corresponding

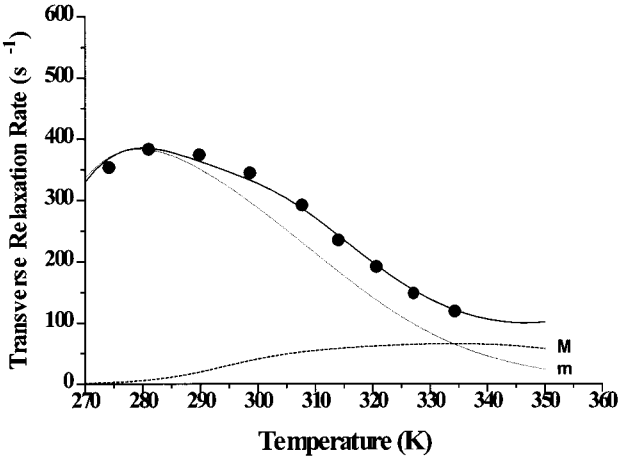

Figure 9. Temperature dependence of the ^{17}O (12 MHz) transverse relaxation rate for a 50 mmol/L aqueous solution of [(*RRRR*)-Gd·**4**]$^-$ at pH 6. The curve through the data has been calculated for a model considering the presence in solution of two isomers, as detailed in the text. The lower curves represent the calculated contributions of the individual isomers m (dotted line) and M (broken line).

Table 7. ^{17}O NMR Best Fitting Parameters for M and m Isomers of [(*RRRR*)-Gd·4]$^-$

	M	m
k_{ex}^{298} ($\times 10^6$ s^{-1})	0.5 ± 0.1	22 ± 2
ΔH_M (kJ/mol)	50 ± 4	72 ± 3
τ_v (ps)	21 ± 4	6 ± 2
ΔH_V (kJ/mol)	48 ± 3	11 ± 1

Eu complexes (ΔG^{isom} (298 K) = -3.5 kJ mol^{-1} for [(*RRRR*)-Eu·**4**]$^-$ relative to the equilibrium M ↔ m). To check the validity of eq 3 and thus the reliability of the kinetic data in Table 6, we fitted the ^{17}O relaxation data to a model that takes into account the presence of two isomeric species characterized by the same values of Δ^2 and A/h and different values of k_{ex}, ΔH_M, τ_V, and ΔH_V. The results are shown in Figure 9, and the parameters are reported in Table 7. The values of the individual water exchange rates for the two isomers are in excellent agreement with those of Table 6 indicating that, the simplified procedure notwithstanding, the results obtained are consistent. Obviously this is also a consequence of the predominance in solution of one (m) of the two isomers.

Conclusions

Values of the water exchange lifetime at gadolinium correlate well with the proportion of the twisted square-antiprismatic (m) complex observed in solution. Exchange is fastest for the (*RRRR*)-[Gd·**4**] complex, which contains the highest proportion of the m isomer in solution. The fact that the faster rate of exchange in the minor isomer (2.1×10^7 s^{-1}, 298 K) is apparently independent of complex structure and intramolecular dynamics suggests that the position of the transition state for dissociative water interchange is late; this may not be the case with the slower exchanging isomer, of course. Evidently, the way forward in designing more effective higher molecular weight contrast agents is to base their structure on established complexes in which the proportion of the isomer which exchanges most rapidly is optimized (e.g., the (*RRRR*)-α-substituted derivatives of dota). Indeed the values of τ_m measured for (*RRRR*)- and (*RRRS*)-[Gd·**4**] at 312 K (16 and 30 ns, respectively) are close to the optimal value of 30−40 ns, suggested by a theoretical analysis.[1a] The outstanding problem then to address in the pursuit of higher molecular weight high-relaxivity agents remains how to efficiently couple the motion of the whole macromolecule to the motion of the paramagnetic center.

Experimental Section

General Information. Reactions requiring anhydrous conditions were carried out using Schlenk-line techniques under an atmosphere of dry argon. Water was purified by the Purite$_{STILL}$-plus TM system. Thin-layer chromatography was carried out on neutral alumina plates (Merck AST 5550) and visualized by iodine staining. Infrared spectra were recorded on a Perkin-Elmer 1600 FT spectrometer using GRAMS-Analyst software; solids were incorporated into KBr disks.

The NMR spectra were acquired using a Brüker AC250 spectrometer operating at 250.13 and 62.9 MHz for ^1H and $^{13}C-\{^1H\}$ measurements, respectively; a Varian VXR 200 operating at 200 MHz for ^1H; a JEOL EX-90 operating at 90 MHz for ^1H and 12 MHz for ^{17}O; a JEOL EX-400 operating at 400 and 100.6 MHz for ^1H and $^{13}C-\{^1H\}$, respectively, and a Varian VXR 400 operating at 399.96 MHz for ^1H. Two-dimensional spectra were run on a JEOL EX-90 and a Varian VXR 200 spectrometer. Variable-temperature ^1H NMR studies were carried out on a Varian VXR 400, a JEOL EX-90, and JEOL EX-400 instrument. Spectra were referenced internally relative to *tert*-butyl alcohol (δ_H 0; δ_C 31.3) for paramagnetic complexes or to the residual protio solvent resonances, relative to TMS.

The longitudinal water proton relaxation rate at 20 MHz was measured by using a Stelar Spinmaster spectrometer (Stelar, Mede (PV) Italy) operating at 0.5 T, by means of the standard inversion−recovery technique (16 experiments, 4 scans). A typical 90° pulse width was 3.5 ms, and the reproducibility of the T_1 data was ±0.5%. The temperature was controlled with a Stelar VTC-91 air-flow heater equipped with a copper constant thermocouple (uncertainty of 0.1 ± °C). The proton $1/T_1$ NMRD profiles were measured on the Koenig-Brown field-cycling relaxometer over a continuum of magnetic field strength from 0.000 24 to 1.2 T (corresponding to 0.01−50 MHz proton Larmor frequency). The relaxometer works under computer control with an absolute uncertainty in $1/T_1$ of ±1%. Variable-temperature ^{17}O NMR measurements were recorded on JEOL EX-90 (2.1 T) spectrometer equipped with a 5-mm probe, by using a D_2O external lock. Solutions containing 2.6% of ^{17}O isotope (Yeda, Israel) were used. The observed transverse relaxation rates were calculated from the signal width at half-height.

For europium complexes, the rate of isomer exchange was assessed on a Varian VXR 400 instrument by saturation transfer methods,[13] measuring the relaxation rate of the axial proton in the minor twisted square-antiprismatic at ∼43 ppm (293 K), using the inversion−recovery method. The integral of this peak was measured in the absence and presence of saturation of the peak due to the equatorial ring proton resonance of the major isomer (at ∼−8.6 ppm). The probe temperature was calibrated using the MeOH chemical shift thermometer (±0.3 K) and the resonance of the other shifted axial ring proton (due to the major isomer) at ∼22 ppm was used as an internal calibrant for the integration measurements.

Electrospray mass spectra were recorded on a VG Platform II (Fisons) instrument, operating in positive ion mode. Details of the instrumentation and data-handling procedures used for determining emission radiative rate constants for Eu and Tb complexes have been described elsewhere.[8c]

Crystallography. Single-crystal X-ray diffraction experiments were carried out at 150 K for the stereoisomers of **4** using a Siemens-SMART three-circle diffractometer (ω-scan mode). Graphite-monochromated Cu Kα radiation (λ = 1.541 84 Å) and an Oxford Cryostream open-flow N_2 gas cryostat was used. Experiments with the Eu, Gd, and Tb complexes of **4** were carried out on a Siemens SMART-CCD diffractometer using graphite monochromated Mo Kα radiation (λ = 0.719 73 A). The structures of the ligands were solved by direct methods, and the complexes were solved by Patterson and Fourier methods and refined by full-matrix least squares against F^2 for all data using SHELXTL software.[26] All non-H atoms, excluding solvent, were refined with anisotropic displacement parameters; all H-atoms were located from difference Fourier maps (or were placed in calculated

positions where necessary) and were refined in isotropic approximation. Data are summarized in Table 1, and atomic coordinates and displacement parameters, bond distances, and angles have been deposited at the Cambridge Crystallographic Data Centre.

1,4,7,10-Tetrakis[(3′-carboxyl)-1′-carboxypropyl]-1,4,7,10-tetraazacyclododecane. To a mixture of 1,4,7,10-tetraazacyclododecane (8 g, 46.5 mmol) and potassium carbonate (12 g, 140 mmol) in dry acetonitrile (100 mL) was added racemic dimethyl α-bromoglutarate (47.8 g, 200 mL), and the mixture was heated at 60 °C for 48 h. Progress of the reaction was monitored by TLC (SiO_2; 60% THF, 30% CH_2Cl_2, 5% MeOH, 5% aqueous ammonia), and the progressive disappearance of the trans diester diastereoisomers (*RR*/*SS* and *RS*) at $R_f = 0.30/0.25$, the triester stereoisomers (*RRR*/*SSS*, *RSR*/*SRS*, *RRS*/*SSR*) with $R_f = 0.55$, was accompanied by formation of the diastereoisomeric mixture of the octamethyl ester ($R_f = 0.82$). The cooled suspension was filtered, solvent was removed under reduced pressure, and the residue was taken up in dichloromethane (50 mL). The organic phase was washed with water (2 × 20 mL) and dried (K_2CO_3), and solvent was removed to leave a viscous pale-yellow gum which was purified by column chromatography on silica gel [CH_2Cl_2, then 30% THF/CH_2Cl_2, and finally 3% MeOH, 0.5% aqueous ammonia in THF/CH_2Cl_2 (1:3)] to yield the octamethyl ester as a pale yellow oil (25.8 g, 69%) which was hydrolyzed without further purification: LRES MS $(M + H)^+$ 805.2; IR(film) 2951, 2847, 1731 (ν_{CO}), 1453, 1251, 1208, 1167, 918, 730 cm^{-1}.

The ester was dissolved in methanol (50 mL), a solution of sodium hydroxide (40 g) in water (200 mL) was added, and the resultant mixture was heated at 70 °C for 18 h. After removal of the methanol under reduced pressure, the solution was treated with 400 g of weak acid ion exchange resin (IRC-H^+), filtered (pH 6.5), and then adsorbed onto a column containing 350 g of an anion exchange resin (IRA-458, OH^- strong). The column was rinsed with water (4 dm^3), and the product eluted with acetic acid (6 M, 2 dm^3). Evaporation of the solvent (azeotropic removal with added toluene) yielded a colorless solid which was dried under vacuum (60 °C, 18 h). Analysis by reversed-phase HPLC (C_{18}, 5 μμ; λ_{obs} 200 nm; 1 mL min^{-1}; 98% H_2O, 0.1% CF_3CO_2H, 1.9% MeCN) revealed three peaks at $t_R = 6.16$ (∼60%), 5.18 (∼20%), and 3.28 (∼20%) min. Fractional crystallization of the mixture of acids (dilute aqueous HCl, pH ∼3) gave successively the product with $t_R = 6.16$ min (*RRRS* + *RRRR* isomers), then $t_R = 5.18$ min (*RRSS*), and finally $t_R = 3.28$ min (*RSRS*). The configuration of the *RRRS* (SSSR), *RSR*,*S* and *RRSS* isomers was established by X-ray analysis of the separated recrystallized (pH 2, dilute HCl) ligands (see Supporting Information for details of the structural analyses).

RRRR(SSSS) isomer: LRES MS $(M - 2H)^{2-}$ 345.1, $(M - H)^-$ 691.1; IR (KBr) 3436 (ν_{OH}), 2920, 1720 (ν_{CO}), 1632 (α-CO_2^-), 1460, 1402, 1366, 1314, 1222, 1088, 1032, 956, 826 cm^{-1}; ^1H NMR (400 MHz, pD 6) δ 1.81 (br m, 8H, CH_2CH), 2.12 (br, 8H, CH_2CO_2H), 3.12 (br m, 16H, CH_2N), 3.42 (br m, 4H, CH); ^{13}C NMR (100 MHz, pD 6) δ 23.9 ($CHCH_2$), 34.4 (CH_2CO), 47.4 (CH_2N), 64.1 (CHN), 175.0, 180.9 (CO).

RRRS(SSSR) isomer: LRES MS $(M - 2H)^{2-}$ 345.1 (100), $(M - H)^-$ 691.2 (43); IR (KBr) 3436 (ν_{OH}), 2919 (ν_{CH}), 1720 (ν_{CO}), 1632 (α-CO_2^-), 1460, 1402, 1366, 1314, 1222, 1088, 1033, 957, 825 cm^{-1}; ^1H NMR (400 MHz, pD 3.5) δ 1.79 (br m, 8H, CH_2CH), 2.41 (br m, 8H, CH_2CO), 3.13 (br m, 16H, CH_2N), 3.63 (br m, 4H, CHN); ^{13}C NMR (100 MHz, pD 3.5) δ 20.4 (CH_2CH), 32.0 (CH_2CO), 32.5 (CH_2CO); 44.7, 45.7, 46.5, 47.1 (CH_2N); 62.3, 63.5 (CH); 173.1, 178.3, 178.5 (CO).

RSRS isomer: LRES MS $(M - 2H)^{2-}$ 345.1 (100), $(M - H)^-$ 691.1 (43); IR (KBr) 3436 (ν_{OH}), 2920, 1720 (ν_{CO}), 1632 (α-CO_2^-), 1460, 1402, 1366, 1314, 1222, 1088, 1032, 956, 826 cm^{-1}; ^1H NMR (400 MHz, pD 3.8) δ 1.3−2.8 (vbr m, 32H, $CH_2N + CH_2CH_2CO_2$), 3.00 (br m, 4H, CHCO); ^{13}C NMR (100 MHz, pD 3.8) δ 19.1 (CH_2CH), 27.4 ($CHCH_2$); 34.9, 36.9 (CH_2CO_2); 44.8, 45.5, 46.2, 46.7 (CH_2N); 63.0, 64.6 (CH); 178.7, 180.9 (CO).

RRSS isomer: LRES MS $(M - 2H)^{2-}$ 345.1 (100), $(M - H)^-$ 691.2 (40); IR (KBr) 3438 (ν_{OH}), 2921, 1720 (ν_{CO}), 1631 (α-CO_2^-), 1461, 1401, 1368, 1315, 1224, 1090, 1031, 956, 824 cm^{-1}; ^{13}C NMR (50 MHz, pD 3.5) δ 24.1, 31.8 (CH_2CH); 39.5, 40.9 (CH_2CO); 48.7, 49.3, 50.6, 51.8 (CH_2N); 67.8, 68.1, 68.4, 69.5 (CH); 185.1, 188.9 (CO).

Representative Procedure for Lanthanide Complex Formation. *H_3O^+[Eu(RRRR/SSSS)·H_4* ***4*** *$(OH_2)]^-$·$2H_2O$*. To a solution of europium nitrate pentahydrate (31 mg, 73 μmol) in water (3 mL) was added (*RRRR*/*SSSS*)-**4** (50 mg, 73 μmol). The pH was adjusted to 5.5 (dilute aqueous sodium hydroxide solution) and the mixture heated at 90 °C for 18 h. Solvent was removed under reduced pressure and the complex recrystallized, at 5−15 °C, from dilute aqueous hydrochloric acid (pH 3.5−4). Colorless crystals of the complex were isolated by filtration (48 mg, 72%): Anal. Calcd for $C_{28}H_{49}EuN_4O_{20}$: C, 36.6; H, 5.34; N, 6.10. Found: C, 36.3; H, 5.59; N, 6.03. LRES MS $(M - H)^-$ 419.1 (100) $(M)^-$ 839.0; ^1H NMR (200 MHz, pD 5.5, 293 K) δ 41.9 (s, 4H, ring CH axial, minor (M) isomer), 22.0 (s, 4H, ring CH axial, major (m) isomer), 4.1 (s, 4H, CHC*H*H′), −0.5 (s, 4H, C*H*H′CO_2), −1.1 (s, 4H, CH*H*′CO_2), −2.0 (s, 4H, CH−CHH′), −3.1 (s, 4H, ring CH equatorial, major isomer), −4.2 (s, 4H, ring CH′ axial, major isomer), −4.9 (s, 4H, ring CH equatorial, minor (M) isomer), −8.6 (s, 4H, ring CH′ equatorial), −12.2 (s, 4H, CH), −25.4 (s, 4H, CH-minor isomer); IR (KBr) 3445 (ν_{OH}), 2984, 2933, 1688 (ν_{CO}), 1598 (ν_{CO}), 1451, 1410, 1315, 1219, 1097, 1076, 983, 920, 880 cm^{-1}. Complexes of Eu and Gd with the other isomers of **4** were prepared in an analogous manner and gave similar IR, LRES MS, and microanalytical data. Partial assignments of the ^1H NMR have been undertaken in each case, aided by $^1H-^1H$ COSY experiments.

H_3O^+[Eu(RRRS/SSSR)·H_4 ***4*** *$(OH_2)]^-$·$2H_2O$*: ^1H NMR (200 MHz, pD 5.4, 293 K) δ 48.1 (s, 1H, ring CH axial, major (M) isomer), 43.8 (s, 1H, ring CH axial, major isomer), 43.0 (s, 1H, ring CH axial, major isomer), 38.0 (s, 1H, ring CH axial, major isomer), 26.8 (s, 1H, ring CH axial minor (m) isomer), 23.5 (s, 1H, ring CH axial, minor isomer), 21.4 (s, 1H, ring CH axial, minor isomer), 20.2 (s, 1H, ring CH axial, minor isomer), 8.0, 4.0, 3.1, 1.1, 0.5, 0.2, −2.0, −3.1, −6.0, −7.9, −9.1, −10.0, −11.3, −14.2, −16.4, −16.8 (1 s, 1H, CHN, major isomer), −27.1 (s, 1H, CHN), −27.6 (s, 1H, CHN), −28.6 (s, 1H, CHN).

H_3O^+[Eu(RSRS)·H_4 ***4*** *$(OH_2)]^-$·$2H_2O$*: ^1H NMR (200 MHz, pD 5.6, 293 K) δ 50.3 (s, 2H, ring CH′ axial, major (M) isomer), 40.1 (s, 2H, ring CH axial, major isomer), 27.3 (s, 2H, ring CH′ axial, minor (m) isomer), 20.3 (s, 2H, ring CH axial, minor isomer), 7.0 (s, 2H, ring CH equatorial, major isomer), 0.1 (s, 2H, ring CH′ equatorial), −1.1 (s, 2H, C$H_aH_bCO_2$), −3.2 (s, 2H, CH_2CO_2), −4.0 (s, 2H, C$H_aH_bCO_2$), −5.3 (s, 2H, ring CH″ axial), −6.2 (s, 4H, CHCH_2), −7.0 (s, 2H, ring CH″ axial), −8.1 (s, 2H, ring CH″ equatorial), −11.3 (s, 2H, CHCH_aH_b), −15.0 (s, 2H, ring CH″ equatorial), −18.1 (s, 2H, CHCH_aH_b), −18.5 (s, 2H, CHN), −28.0 (s, 2H, CH′N).

H_3O^+[Eu(RRSS)·H_4 ***4*** *$(OH_2)]^-$·$2H_2O$*: ^1H NMR (200 MHz, pD 5.5, 293 K) δ 50.5 (s, 1H, ring CH axial, major (M) isomer), 46.4 (s, 1H, ring CH axial, major isomer), 45.9 (s, 1H, ring CH axial, major isomer), 40.4 (s, 1H, ring CH axial, major isomer), 8.1 (s, 1H, ring CH equatorial), 3.9 (s, 1H, ring CH equatorial), 2.0 (s, 1H, ring CH equatorial), 1.6 (s, 1H, ring CH equatorial), −0.6 to −6.1 (mult, 16H, CH_2CH_2 + CH′ axial), −8.0 to −13.0 (mult, 6H, ring CH equatorial + CHCH_2), −17.5 (s, 1H, CHCH_2), −18.0 (s, 1H, CHCH_2); −18.2, −19.1, −27.2, −28.9 (s+s+s+s, 4H, CHN).

Formation of H_3O^+[Ln(RRRR/SSSS)·H_4 ***4*** *$(OH_2)]^-$·nH_2O*. Ytterbium oxide (12 mg, 30 μmol) and (*RRRR*)-**4** (40 mg, 58 μmol) were added to water (5 mL). The suspension was heated with stirring at 90 °C for 12 h, maintaining the pH in the range 2−3 for the first 6 h and then at 5.5 thereafter. The mixture was filtered, solvent removed under reduced pressure, and the residue crystallized slowly by controlled evaporation from dilute aqueous hydrochloric acid at 40 °C and pH 2.5 to yield colorless crystals (40 mg, 72%): Anal. Calcd for $C_{28}H_{51}YbN_4O_{21}$: C, 35.1; H, 5.32; N, 5.85. Found: C, 34.9; H, 5.60; N, 5.56. LRES MS $(M - H)^-$ 430 (100), $(M)^-$ 860 (83); ^1H NMR (200 MHz, pD 5, 293 K) δ 157.5 (s, 4H, ring axial CH, minor (M) isomer), 100.1 (s, 4H, ring CH axial, major (m) isomer), 29.7 (s, 4H, ring CH equatorial, minor (M) isomer), 24.0 (s, 4H, ring CH equatorial, minor isomer), 18.0 (s, 4H, ring CH equatorial, major isomer), 11.9 (s, 4H, ring CH equatorial, major isomer), −9.6 (s, 8H, CH_2CO_2), −13.0 (s, 4H, CH*H*′CH_2, major isomer), −18.6 (s, 4H, C*H*H′CH_2, major isomer), −21 to −24 (s+s+s, 16H, $CH_2CO_2H + CH_2CH_2$, minor isomer), −37.8 (s,

4H, ring CH′ axial, major isomer), −51.0 (s, 4H, ring CH′ axial, minor isomer), −74.0 (s, 4H, NCH major isomer), −115.7 (s, 4H, NCH, minor isomer).

Complexes of Pr, Ho, and Tb with the racemic, C_4-symmetric isomer (*RRRR*/*SSSS* at C) were prepared in an analogous manner and gave LRES MS and microanalytical data in accord with the proposed structures. The ratio of the two isomers in solution (m/M:twisted square-antiprismatic/square-antiprismatic) was measured by integration of the most shifted ring axial proton resonance, e.g., for the Tb complex at −410 (m) and −476 ppm (M); for Pr at −35.6 (m) and −52 ppm (M), giving m/M ratios of 20:1 (Pr), 8:1 (Nd), 4:1 (Eu), 1.5:1 (Tb), 4:1 (Ho) and 15:1 (Yb).

Acknowledgment. We thank the EPSRC, the Royal Society (Leverhulme Trust Senior Research Fellowship, D.P.), the BBSRC, the EU-COST D-18 program for support and the reviewers for helpful comments.

Supporting Information Available: Various data X-ray, ^{17}O-NMR and NMRD as listed in the text. This material is available free of charge via the Internet at http://pubs.acs.org.

JA994492V